Food Chemistry: X 26 (2025) 102230

Contents lists available at ScienceDirect

Food Chemistry: X

journal homepage: www.sciencedirect.com/journal/food-chemistry-x

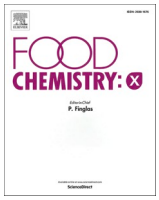

Proteomics integrated with metabolomics: Analysis of the internal mechanism underlying changes in meat quality in different muscles from bactrian camels

Rendalai Si [a], Liang Ming [a], Xueyan Yun [a], Jing He [a], Li Yi [a], Qin Na [a], Rimutu Ji [a,b,*], Tungalag Dong [a,*]

[a] College of Food Science and Engineering, Inner Mongolia Agricultural University, 306 Zhaowuda Road, Hohhot, Inner Mongolia 010018, China
[b] Inner Mongolia Institute of Camel Research, Alxa 737300, China

ARTICLE INFO

Keywords:
Proteomics
Metabolomics
Bactrian camels
Muscles
Meat quality

ABSTRACT

Knowledge about the quality of meat obtained from different muscles is crucial for developing high-quality camel meat for commercial use. Metabolomic and proteomic profiles of the longissimus thoracic (LT), semitendinosus (ST), and psoas major (PM) muscles of the bactrian camel, which significantly vary in aspects such as intramuscular fat (IMF) content and shear force, were comprehensively compared to evaluate the impact of these changes on meat quality. Compared with ST and PM muscles, LT muscles had higher IMF content, were more tender, and had a lower shear force. Proteomic analysis unveiled significant differences in metabolic enzymes and binding proteins among different muscles. Based on correlation analysis, 20 key proteins and metabolites closely related to meat quality were screened. Integration of proteomic and metabolomic data highlighted oxidative phosphorylation, TCA cycle, and glycolysis as key distinguishing pathways among different muscles. These results offer effective information for producing high-quality camel meat.

1. Introduction

Bactrian camels (*Camelus bactrianus*) are among the few large livestock that adapts to the harsh environments of arid and semi-arid regions (Zarrin et al., 2020). Being a precious biological resource, camels can adapt to hostile conditions, such as high temperature, severe cold, drought, food scarcity, and high radiation, better than the other livestock. They have less fat in the body and developed muscles (Burger et al., 2019). Bactrian camel meat, as a product with national geographical indication, is primarily produced in China's northwest regions (Si, Na, et al., 2022).

With recent improvements in people's living standards, consumers' concepts have also changed from simply viewing meat products as a source of basic nutrients to considering it a health-promoting supplement (Kadim et al., 2008; Kadim et al., 2022). Therefore, the demand for meat products with high nutritional and health value has increased (Baba et al., 2021). Camel meat is a high-protein meat with low fat and cholesterol and is rich in various polyunsaturated fatty acids and amino acids. Therefore, it is increasingly favored by the market (Kadim et al., 2018; Suliman et al., 2020). Moreover, camel meat is believed to possess medicinal properties. According to some studies, camel meat has been traditionally used to remedy various diseases such as sciatica, hyperacidity, cardiovascular diseases, hypertension, pneumonia, and respiratory diseases (Kadim et al., 2022; Kurtu, 2004). Hence, the health profile of camel meat products in China is a promising future prospect as a tool for augmenting the value of this functional meat.

The quality characteristics of camel meat varies according to age, sex, muscle type, breed type, and feeding conditions of the animal (Al-Owaimer et al., 2014; Kadim et al., 2006). Of them, muscle type is a crucial factor affecting the quality of camel meat (Kadim et al., 2013). Current analyses of quality traits of individual muscles in beef, pork, and sheep have revealed that specific muscles can be marketed more successfully on an individual basis (Cheng et al., 2020; Tschirhart-Hoelscher et al., 2006). The marketing of individual muscles may boost the demand for camel meat products. Such a marketing system requires having more information regarding the nutritive value of those individual muscles. Most current studies on camel meat have focused on aspects such as muscle fibers, tenderness, color, water-holding capacity,

* Corresponding author at: College of Food Science and Engineering, Inner Mongolia Agricultural University, 306 Zhaowuda Road, Hohhot, Inner Mongolia 010018, China.
E-mail addresses: yeluotuo1999@vip.163.com (R. Ji), dongtlg@imau.edu.cn (T. Dong).

https://doi.org/10.1016/j.fochx.2025.102230
Received 7 October 2024; Received in revised form 28 December 2024; Accepted 24 January 2025

processing characteristics, and nutritional components (Kadim et al., 2006; Si, Wu, et al., 2022; Lyu et al., 2024). However, few studies have investigated nutrient metabolism and internal factors that affect the quality of camel meat from different muscles.

The longissimus thoracic (LT) is the most commonly investigated muscle in meat studies (Si, Na, et al., 2022). It contains a relatively high level of intramuscular fat (IMF) and shows better tenderness. Conversely, the semitendinosus (ST) demonstrates relatively inferior tenderness, characterized by thicker muscle fibers and a greater quantity of connective tissue, which induces a higher shear force (Kadim et al., 2022). The psoas major (PM) is noted for its high juiciness. It has a low fat content but a relatively high moisture content. Its fine muscle fibers allow it to retain moisture more effectively during the chewing process, thus presenting higher juiciness (Suliman et al., 2020). For these reasons, the present study investigated these three muscles from nutritional, quality, and economic viewpoints.

To determine exactly what changes occur in the quality traits of muscles from different parts, we considered using omics methods. Metabolomics and proteomics are valid methods for identifying metabolites, proteins, and related pathways (Fan et al., 2018; Hwang et al., 2023; Rozanova et al., 2021). Proteomics is a valuable method used in meat science research. This method can explain the potential biological pathways and molecular mechanisms underlying different quality traits of meat (Huang et al., 2020; López-Pedrouso et al., 2023). Furthermore, metabolomics is primarily used in meat science for studying various aspects, such as meat safety (Zhang et al., 2021), meat quality (Zhang et al., 2022), meat traceability (Chatterjee et al., 2019), and different processing methods (Li et al., 2021) and storage conditions of meat products (Liu et al., 2022). Recent advances in metabolomics and proteomics technologies have largely accelerated the identification and characterization of natural products and their associated metabolites. Therefore, integrated metabolo-proteomics, conducted using ultra-high-performance liquid chromatography coupled to tandem mass spectrometry (UPLC-MS/MS), is a good approach for identifying metabolites or proteins that may affect the quality characteristics of camel muscles.

We here performed an integrated untargeted metabolomics and tandem mass tag (TMT)-based proteomic analysis to comprehensively understand the variations in the quality of meat from the various muscles of camel and the reasons underlying these variations. We also sought to identify the key regulatory pathways and proteins responsible for the alterations in the metabolites and quality characteristics of camel meat.

2. Materials and methods

2.1. Animals and sample collection

The six male Alxa bactrian camels (age: 3.5 years, mean weight: 424 ± 12 kg) were provided by Lifa Agriculture and Animal Husbandry Industry Co., Ltd., Inner Mongolia, China. The Animal Administration and Ethics Committee of the Camel Protection Association of Inner Mongolia reviewed and approved the experimental protocol (Permit No. 2021–003). All animals were kept under the same environmental and management conditions for 3 months to attain a similar nutritional background before slaughter.

Following standard commercial procedures, the experimental animals were fasted for 12 h and slaughtered at an abattoir (Lifa Agriculture and Animal Husbandry Industry Co., Ltd., Inner Mongolia, China) according to the food industry-approved Halal food quality-certified protocols guided by the tenets of Islam (Al-Owaimer et al., 2014). The ambient temperature at the slaughterhouse ranged between 25 and 27 °C. Three muscles, namely LT, ST, and PM, were collected from the left side of the animal carcasses. Fig. 1 illustrates the specific locations of each muscle. The samples were vacuum packaged (Packaging Sealing Machine, QT-124, China) in polyvinylidene chloride bags (Zhenzhun Biotechnology Co., Ltd., Shanghai, China; pore size 8 cm, thickness 70 μm, O_2 diffusion rates 0.05 $cm^3 \cdot m^2 \cdot d^{-1}$) and stored at −20 °C for further quality measurements (Yu, Tian, et al., 2023). Approximately 5 g meat was collected from each muscle, immediately frozen in liquid nitrogen, stored at −80 °C in a refrigerator (DW-86 L626, Haier, China), and then used for protein and metabolite extraction. For the convenience of statistical data analysis, the abbreviations LT, PM, and ST were used to represent the three muscles, respectively, in this study.

2.2. Meat quality analysis

Meat quality, including intramuscular fat (IMF), pH, shear force, and color values (a^* for redness, L^* for lightness, and b^* for yellowness), was determined by referring to previous methods (Si, Na, et al., 2022). Muscle samples were thawed overnight at 4 °C before the measurements

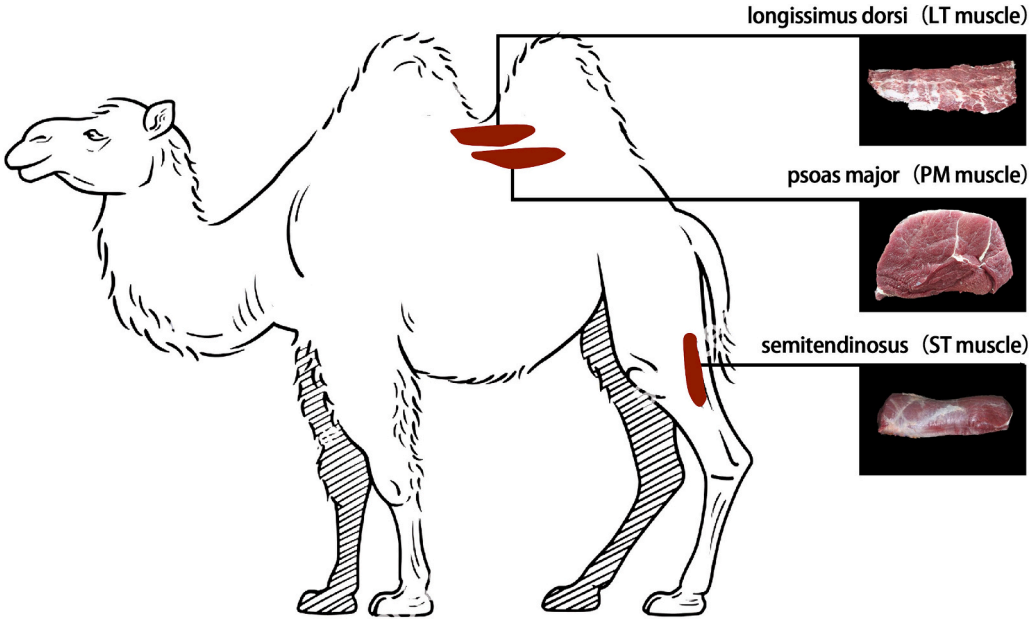

Fig. 1. Location diagram of muscles in three different parts.

were conducted. IMF contents were determined following the Chinese recommended standard (GB/5009.6–2016) according to previous methods (Yu, Wang, et al., 2023). The Chinese recommended standard (GB5009.237–2016) method was used to determine the ultimate pH value of the camel meat as follows: The meat sample was chopped to form minced meat. Minced meat weighing 10.0 g was added to 90 mL water and homogenized (with an Ultra Turrax T25 homogenizer) for 30 min. The pH of the filtrate was measured using a pH meter equipped with a glass electrode (FE28 Benchtop pH Meter, Mettler-Toledo, Leicester, UK). The pH meter was calibrated with pH 4.01 and 6.86 buffers at 22 °C. The color values were measured using a chromameter (Konica Minolta, CR-400, Tokyo, Japan). The determination was based on previous methods (Kadim et al., 2013; Si, Wu, et al., 2022). Approximately 40 min after exposing the fresh surface of the muscle samples, reflectance measurements were recorded. The chromameter was configured to the L^*, a^*, and b^* color spaces, along with illuminant D65, an observer angle of 2°, and an aperture size of 5.0 mm with a closed cone. The chromameter was calibrated using a standardized white tile before measurement. The shear force of the meat samples was assessed using a previous procedure (Biffin et al., 2020). Three different muscles were randomly selected and assigned to a cooking batch. The shear force value was determined as the maximum force (N) perpendicular to the fibers by using a TA-XT ExpressC Texture Analyzer (Weixun Super Technology Co., Ltd., Beijing, China) fitted with a Warner–Bratzler attachment. The parameters were set as follows: the pre-test and post-test speed values were 2 and 2 mm/s, respectively; the test distance was 20 mm; and the trigger force was 5 g. Three readings were taken for all the determinations, and the mean value was calculated.

2.3. TMT analysis methods

2.3.1. Protein extraction

Following Hou et al.'s method, proteins were extracted through TCA/acetone precipitation and the SDT lysis method (Hou et al., 2020). Approximately 2 mL of the protein solution was extracted from each sample by using the SDT lysis method. In this method, the RIPA working solution (comprising 1 % SDS, 1 % Nonidet P40 lysis solution, 1 % sodium deoxycholate, 15 mmol/L NaCl, and 25 mmol/L Tris-HCl, pH 7.6) was added to the sample. Then, the sample was centrifuged at 12,000 ×*g* for 15 min at 4 °C to extract the protein.

2.3.2. Protein digestion

The filter-aided sample preparation enzymatic hydrolysis method was used to hydrolyze the extracted proteins. The obtained proteins were added to an ultrafiltration tube and dissolved with trypsin powder added to 50 mmol/L ammonium bicarbonate. Trypsin was added according to the protein:enzyme mass ratio of 50:1. The ultrafiltration tube was sealed with a sealing film and incubated in an oven at 37 °C for 16–18 h. Then, the digested peptides of each sample were desalted using C18 cartridges (XBridge BEH C18 XP Column (150 mm × 2.1 mm, 1.8 μm), Waters, Milford, MA, USA), concentrated through vacuum centrifugation, and redissolved in 40 μL of 0.1 % (*v*/v) formic acid (FA). Subsequently, the protein content was measured using a BCA Protein Assay Kit (Bio-Rad, USA), and the sample was stored at −80 °C.

2.3.3. TMT labeling

Each TMT reagent was dissolved in 70 μL ethanol and added to the respective peptide mixture for labeling. For each sample, 100 μg of the peptide mixture was labeled with the 9-plex TMT reagent (TMT Mass Tagging Kits and Reagents, Thermo Fisher Scientific, MA, USA). The samples were labeled as (PM-1)-127 N, (PM-2)-128 N, (PM-3)-130C, (LT-1)-128C, (LT-2)-127C, (LT-3)-129C, (ST-1)-131, (ST-2)-130 N, and (ST-3)-129 N; multiplexed; and vacuum dried.

2.3.4. High-pH reverse-phase fractionation

Reverse-phase UPLC was performed to segregate the TMT-labeled digested samples into 12 fractions by using an increasing acetonitrile step-gradient elution.

2.3.5. Mass spectrometry

Each fraction was injected for the Nano LC-MS/MS analysis. For each sample, 1 μg total peptides was separated and analyzed using a Nano-UPLC system (EASY - nLC1200, Thermo Scientific, USA) coupled to a Q Exactive HFX Orbitrap instrument (Thermo Fisher Scientific, USA) with a Nano-electrospray ion source. The peptides were separated using a reversed-phase column (ReprosilPur 120 C18 AQ, 1.9 μm, Dr. Maisch (100 μm × 15 cm), Germany). Mobile phase A was H_2O with 0.1 % FA and 2 % acetonitrile (ACN), and mobile phase B was 80 % ACN and 0.1 % FA. The sample was separated with a 90-min gradient at a 300 nL/min flow rate. Gradient B: 2 %–5 % for 2 min, 5 %–22 % for 68 min, 22 %–45 % for 16 min, 45 %–95 % for 2 min, and 95 % for 2 min.

Data-dependent acquisition (DDA) was performed in the profile and positive mode by using an Orbitrap analyzer at 120,000 (@200 *m/z*) resolution and an m/z range of 350–1600 for MS1. The resolution for MS2 was set to 45,000, with a fixed first mass of 110 m/z. The automatic gain control targets for MS1 and MS2 were set to 3e6 and 1e5 with max IT of 30 and 96 ms, respectively. HCD fragmented the top 20 most intense ions with a normalized collision energy of 32 % and isolation window of 0.7 m/z. The dynamic exclusion time window was 45 s. Single-charged peaks and peaks with a charge of >6 were excluded from the DDA procedure (Müller 2020).

2.3.6. Database search and data analysis

MS/MS spectra were processed using Proteome Discoverer software (Version 2.4.0.305, Thermo Fisher Scientific) and the built-in Sequest HT search engine. The MS spectra lists were searched against their species-level UniProt FASTA databases (uniprot-Camelus_9836–2021-5.fasta). During this search, carbamidomethyl [C], TMT 6 plex (K), and TMT 6 plex (N-term) were used as fixed modifications, and oxidation (M) and acetyl (protein N-term) were used as variable modifications. Trypsin was used as a protease. A maximum of two missed cleavage(s) was allowed. The false discovery rate was set to 0.01 for PSM and peptide levels. The peptides were identified with an initial precursor mass deviation of up to 10 ppm and a fragment mass deviation of 0.02 Da. Unique peptides and razor peptides were used for quantifying the proteins, and normalization was achieved with the total peptide amount. To determine significant changes in protein expression, a fold change (FC) of >1.5 or < 0.67 and $P < 0.05$, as determined using Student's *t*-test, were established as cut-off values.

2.4. Untargeted metabolomic analysis methods

2.4.1. Metabolite extraction

In this experiment, preprocessing was performed according to Dunn et al.'s method (Dunn et al., 2011). Each sample from each group was approximately 50 mg in weight. To extract metabolites, 1000 μL methanol:acetonitrile:water (2:2:1, *v/v*) was added to the samples, vortexed for 60 s, homogenized at 35 Hz for 4 min, and sonicated for 5 min in an ice water bath. The homogenization and sonication cycle was repeated three times. The samples were centrifuged at 12,000 rpm, 4 °C for 15 min. The supernatant was dried in a vacuum centrifuge, transferred to a new tube, and stored at −80 °C. To monitor the stability and repeatability of the instrument analysis, an equal aliquot of supernatants from all samples was mixed to prepare the quality control sample. Each sample had six biological replicates, thus totaling to 18 samples.

2.4.2. LC-MS/MS analysis

LC-MS/MS analyses were performed using a UHPLC system (Vanquish, Thermo Fisher Scientific) with a UPLC BEH Amide column (2.1 mm × 100 mm, 1.7 μm, Waters, Ireland) coupled to a Q Exactive

HFX mass spectrometer (Orbitrap MS, Thermo Fisher Scientific). Mobile phase A consisted of 25 mmol/L ammonium acetate and 25 mmol/L ammonia hydroxide in water (pH = 9.75), and mobile phase B contained the same compounds in acetonitrile instead of water. The autosampler temperature and injection volume were 4 °C and 3 μL, respectively. The QE HFX mass spectrometer was used to acquire the MS/MS spectra in an information-dependent acquisition mode in the control of the acquisition software (Xcalibur, Thermo). The ESI source conditions were as follows: sheath gas flow rate, 30 Arb; Aux gas flow rate, 25 Arb; capillary temperature, 350 °C; full MS resolution, 60,000; MS/MS resolution, 7500; collision energy, 10/30/60 in the NCE mode; and spray voltage, 3.6 kV (positive) or − 3.2 kV (negative).

2.4.3. Data processing and statistical data analysis

Raw data were converted into the mzXML format by using ProteoWizard and processed using an in-house program (Shanghai Biotree Biomedical Technology Co., Ltd) for peak detection, extraction, alignment, and integration. This program was developed using R and based on XCMS. Then, metabolites were annotated by referring to the MS2 database (BiotreeDB, V2.1). The cutoff for annotation was set at 0.3. SIMCA-P (version 14.1, Umetrics, Umea, Sweden) was employed for the multivariate statistical analysis. After Pareto scaling, principal component analysis (PCA), partial least squares-discriminant analysis (PLS-DA), and orthogonal partial least-squares discriminant analyses (OPLS-DA) were performed. Response permutation testing was used to evaluate the model's robustness. Meanwhile, Microsoft Excel 2010 (Microsoft Corp., Redmond, WA, USA) was used to organize the experimental data. The results were statistically analyzed using IBM SPSS Statistics 26.0 (IBM Corp., Armonk, NY, USA). Origin Lab software version 2021 (Origin Lab, Northampton, MA, USA) was used for creating graphs. The significantly different metabolites were identified based on both a significant threshold of variable influence on the projection (VIP) values derived from the OPLS-DA model and *P* values derived from Student's *t*-test on raw data. Metabolites having VIP $>$ 1.0 and $P < 0.05$ were considered significant.

2.5. Bioinformatics analysis

To determine the functional classification and biological properties of the selected differentially expressed proteins (DEPs), the identified protein sequences were mapped using Gene Ontology (GO) terms. Moreover, all DEPs and differentially expressed metabolites (DEMs) were queried by referring to the online Kyoto Encyclopedia of Genes and Genomes (KEGG, http://www.kegg.jp/) database and mapped to KEGG pathways. The enrichment analysis was conducted to explore the effect of DEPs and identify the internal connections between DEPs and metabolic pathways. Only functional categories and pathways with $P < 0.05$ were considered to exhibit significant enrichment. The significantly different metabolites and proteins identified among the three muscles were applied to enquire the integrated KEGG metabolites and proteins by using an R-based software tool for omics data integration.

2.6. Statistical analysis

Microsoft Excel 2010 (Microsoft Corp., Redmond, WA, USA) was used to organize the experimental data. The meat quality indicator data were analyzed using one-way ANOVA with IBM SPSS Statistics 26.0 statistical software (IBM Corp., Armonk, NY, USA). The mean differences were compared using Duncan's multiple range t-test. Comparisons with $P < 0.05$ were considered significant. Data are presented as the mean ± standard errors of at least three independent replicates.

3. Results

3.1. Quality traits of different camel muscles

To assess the quality traits of different muscles, the primary meat quality indices were determined and recorded (Table 1). Significant differences in IMF content were observed among the three muscles ($P < 0.05$). Specifically, the IMF content was considerably higher in the LT muscle than in both the ST and PM muscles. The ultimate pH analysis revealed that the LT and ST muscles had higher pH values than the PM muscle ($P < 0.05$), whereas no differences were observed between the LT and ST muscles. The LT and PM muscles had a significantly lower shear force than the ST muscles ($P < 0.05$). The color indicator analysis showed that L^* values were significantly higher in the PM muscle than in the LT and ST muscles. However, no significant difference in b^* and a^* values was observed among the three muscles.

3.2. Proteomic profiles of different camel muscles

3.2.1. Protein identification and quantification

The TMT combined with UHPLC-QE-MS method was used to isolate and identify proteins from the three muscles. Then, the proteome profiles were assessed. In total, 3415 proteins and 23,227 peptides were recognized with 1 % FDR. Fig. S1 presents the protein quantification results.

3.2.2. Analysis of DEPs

Of the 3415 proteins, those with $P < 0.05$ and FC $\geq$ 1.5 or FC $\leq$ 0.67 were considered DEPs. The PM vs LT group had 141 DEPs, the PM vs ST group had 196 DEPs, and the LT vs ST group had 436 DEPs. Among the DEPs, 102, 128, and 190 DEPs were upregulated in the three muscle groups, whereas 39, 68, and 246 DEPs were downregulated (Fig. 2A). The PCA scatter plot demonstrated strong cluster formations for the three comparison groups. Clear separations were observed between the samples (Fig. 2B). Furthermore, the classification heatmap of all proteins was created (Fig. 2C). According to the heatmap, the ST muscle exhibited opposite upregulation and downregulation of expression compared with the PM and LT muscles, and this phenomenon was consistent with the PCA results.

3.2.3. GO functional classification of DEPs

The protein functional analysis was conducted using all DEPs based on the GO category enrichment and GO and UniProt databases. In total, 552 significant DEPs were classified into the biological process (BP),

Table 1
Means and standard errors for meat quality characteristics of Psoas major, Longissimus thoracic, and semitendinosus muscle samples from Alxa bactrian camels.

Measurement	muscle		
	psoas major (PM)	longissimus thoracic (LT)	Semitendinosus (ST)
Intramuscular fat content (g/100 g)	1.22 ± 0.23 ^{b}	3.66 ± 1.22 ^{a}	0.40 ± 0.12 ^{c}
Ultimate pH	5.58 ± 0.19 ^{b}	6.03 ± 0.29 ^{a}	6.11 ± 0.31 ^{a}
Shear value (N)	85.34 ± 2.96 ^{b}	81.33 ± 2.12 ^{b}	93.43 ± 2.77^{a}
Color parameters			
L^* (lightness)	39.80 ± 1.11 ^{a}	38.65 ± 1.65 ^{ab}	36.87 ± 1.98 ^{b}
a^* (redness)	17.11 ± 0.79 ^{a}	17.68 ± 1.59 ^{a}	17.30 ± 1.12 ^{a}
b^* (yellowness)	8.17 ± 0.43 ^{a}	9.63 ± 2.73 ^{a}	8.41 ± 1.33 ^{a}

a,b: Means ± SD within rows with different superscript letters indicating significant differences ($P < 0.05$).

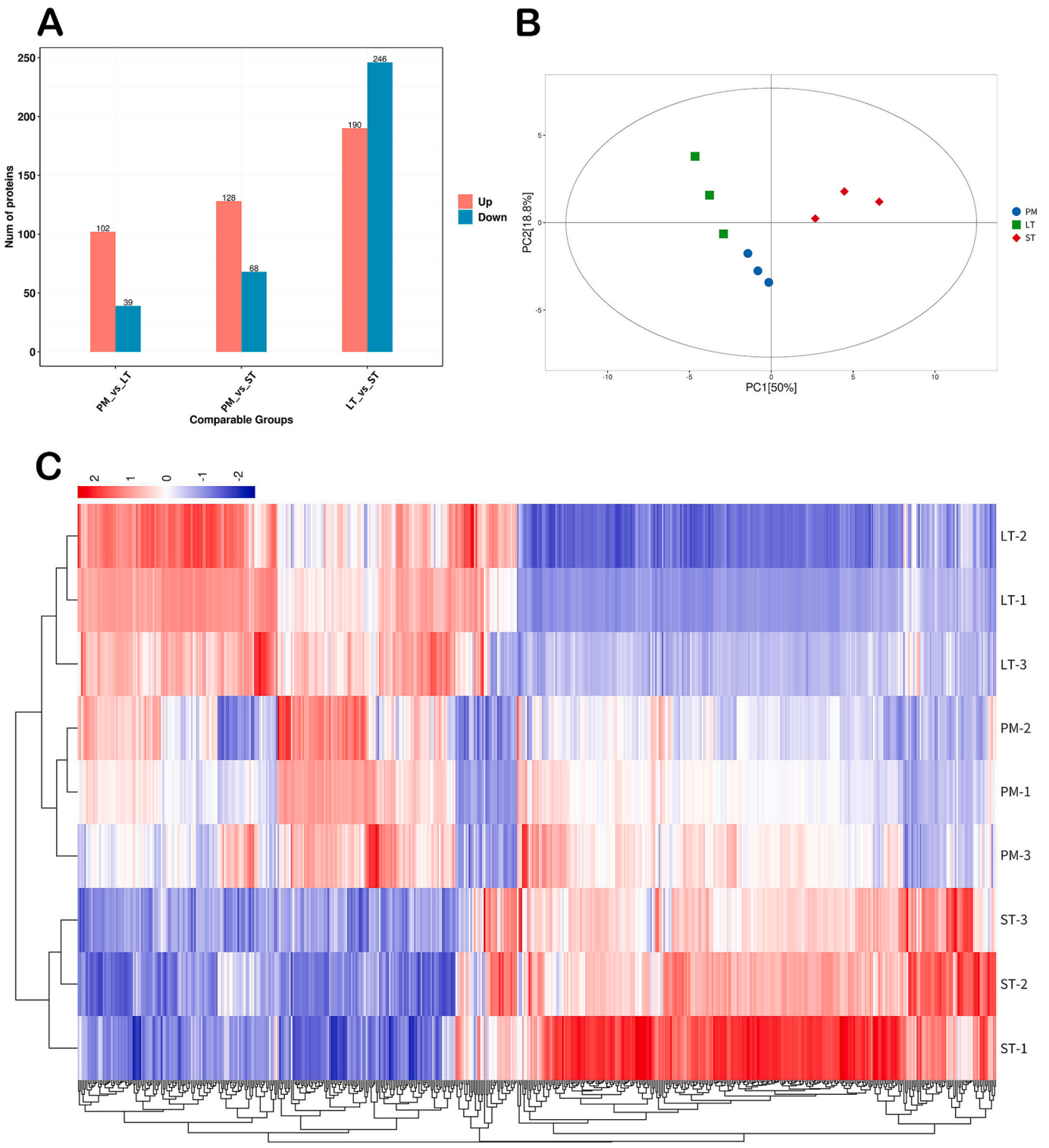

Fig. 2. Analysis of differentially expressed proteins (DEPs).
(A) Number of DEPs in different muscles of camel meat. **(B)** PCA scores of camel meat samples from different muscles. **(C)** Clustering heatmap of DEPs in camel meat samples from different muscles. The abbreviations LT, PM, and ST represent longissimus thoracic, psoas major, and semitendinosus, respectively.

cellular component (CC), and molecular function (MF) categories (Fig. S2). The analysis revealed that metabolic enzyme activity and binding proteins differed significantly among the three comparison groups (Fig. S2A, S2B, S2C), especially in the functional enrichment of NADH dehydrogenase activity, oxidoreductase activity, and phosphoglycerate kinase activity. Moreover, the BP functions of these proteins were predominantly concentrated in oxidation-reduction, nucleotide phosphorylation, glycolysis, and carbohydrate degradation metabolism processes.

3.2.4. *KEGG pathway analysis of DEPs*

As shown in Fig. 3A, in the PM vs LT group, 49 DEPs were assigned to 71 pathways. Of them, 23 pathways were significantly enriched in both groups ($P < 0.05$). The pathway terms exhibiting significance primarily

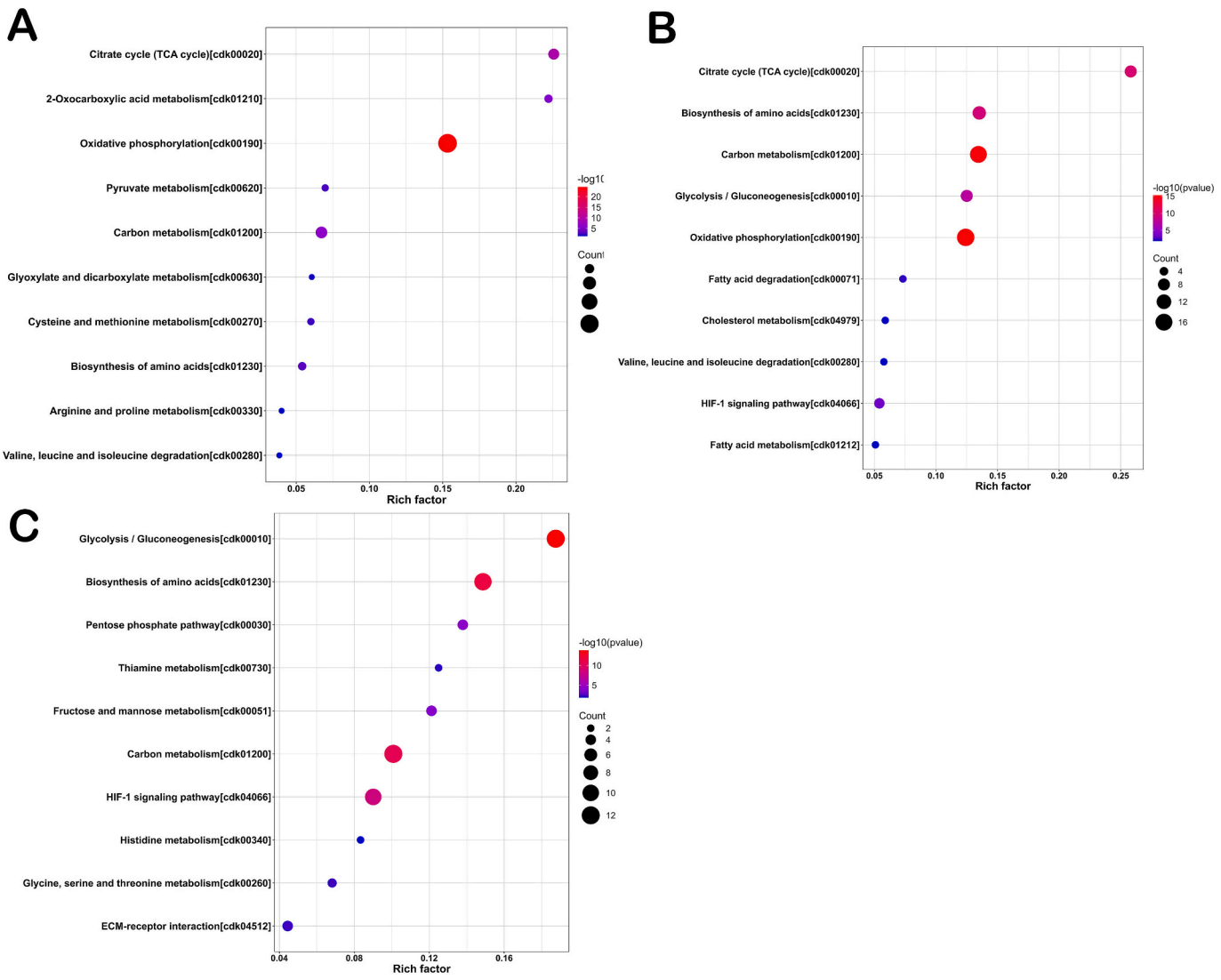

Fig. 3. Bubble diagram of KEGG metabolic pathway enrichment analysis of DEPs.
A, **B,** and **C** represent the comparison groups of PM vs LT, LT vs ST, and PM vs ST, respectively. The abbreviations LT, PM, and ST represent longissimus thoracic, psoas major, and semitendinosus, respectively.

included oxidative phosphorylation (21 DEPs), the citrate cycle (TCA cycle, 7 DEPs), and carbon metabolism (8 DEPs). In total, 40 pathways were significantly enriched in the LT vs ST group ($P < 0.05$; Fig. 3B). The pathway terms displaying significance mainly included oxidative phosphorylation (17 DEPs), the citrate cycle (TCA cycle, 8 DEPs), and glycolysis (8 DEPs). In all, 25 metabolic pathways were significantly enriched in the PM vs ST group ($P < 0.05$) (Fig. 3C) and predominantly included glycolysis (12 DEPs), amino acid biosynthesis (11 DEPs), carbon metabolism (12 DEPs), and the HIF-1 signaling pathway (10 DEPs).

3.2.5. *Protein–protein interaction analysis*

Protein–protein interaction (PPI) networks were further established for DEPs by referring to the STRING database (Fig. S3). In the PM vs LT group, the PPI network of DEPs consisted of 35 nodes and 538 connecting lines, namely 35 proteins and 538 interaction relationships (Fig. S3A). Of them, NDUFV1 (A0A5N4BYD0) had the strongest interaction with 23 proteins, and ND1 (A0A3Q9E313), ND4 (A0A193BM45), and S9YIR5 interacted with 22 proteins. In the LT vs ST group, A0A5N4E712, S9WP04, A0A5N4E712, A0A1D8GWZ9, and S9XMC4 DEPs had strong interactions with other proteins (Fig. S3B). In the PM vs ST group (Fig. S3C), 17 proteins and 26 interactions were observed. Laminin B2 (S9WE42) interacted with 5 proteins, and laminin protein β1 (S9WZC8) interacted with 3 proteins.

3.3. *Analysis of correlation between meat quality indicators and DEPs*

Based on the correlation analysis of the relative quantitative values of 20 DEPs and meat quality indicators, 17, 17, 3, and 13 DEPs were significantly associated with the IMF, shear force, pH, and color values (L^*, b^*, and a^*) of meat, respectively (Table 2). Among them, A0A5N4DL79, A0A5N4DSC6, S9XA78, P68230, S9X3X9, and S9XYY2 were significantly correlated with IMF ($r = 0.979$, 0.979, 0.954, 0.979, 0.946 and 0.946; $P < 0.01$) and shear force ($r = -0.967$, -0.950, -0.950, -0.933, and -0.933; $P < 0.01$), respectively. A0A5N4CQY0, A0A5N4E9R0, and A0A5N4CXA5 were significantly correlated with the pH value ($r = 0.733$, 0.700, and -0.817), respectively; $P < 0.05$). Ten DEPs, namely A0A5N4DTY9, A0A5N4EKQ6, A0A5N4EGJ1, A0A5N4EGP9, A0A5N4DVE1, A0A5N4D8E9, A0A5N4C7V2, A0A5N4CCY6, T0NNA3, and S9WC05, were significantly correlated with IMF, shear force and L^* values ($P < 0.05$). In addition, an extremely significant correlation was observed between the DEPs of A0A5N4E9R0 and A0A5N4CXA5 and b^* ($r = 0.867$ and -0.833; $P < 0.01$).

Table 2
Pearson's correlation between DEPs and quality traits of camel meat in different muscles.

No.	Protein	Description	Intramuscular Fat	Shear force	PH	L^*	a^*	b^*
1	A0A5N4DTY9	Cadherin-5	−0.709*	0.740*	−0.059	−0.706*	−0.101	−0.420
2	A0A5N4EKQ6	Serotransferrin	0.686*	−0.717*	−0.017	0.750*	0.000	0.333
3	A0A5N4EGJ1	Complement factor I	0.720*	−0.733*	0.050	0.717*	0.100	0.433
4	A0A5N4EGP9	Vitamin D-binding protein	0.762*	−0.817*	0.000	0.717*	−0.100	0.350
5	A0A5N4DVE1	Laminin subunit alpha-2	−0.711*	0.750*	0.083	−0.800*	0.050	−0.300
6	A0A5N4D8E9	Collagen alpha-1 chain	−0.711*	0.750*	0.083	−0.800*	0.050	−0.300
7	A0A5N4C7V2	Heat shock protein beta-2	0.661*	−0.733*	−0.033	0.700*	−0.017	0.317
8	A0A5N4CCY6	Ankyrin repeat domain-containing protein 23	0.686*	−0.717*	−0.017	0.750*	0.000	0.333
9	T0NNA3	APOBEC-like N-terminal domain-containing protein	−0.778*	0.733*	0.333	−0.817*	0.117	−0.117
10	S9WC05	Carbonic anhydrase	0.879**	−0.833*	−0.083	0.700*	−0.017	0.333
11	A0A5N4CQY0	Guanylyl cyclase-activating protein 2	−0.201	0.233	0.733*	−0.783*	0.283	0.383
12	A0A5N4E9R0	Gelsolin	0.644	−0.583	0.700*	−0.050	0.433	0.867**
13	A0A5N4CXA5	Myosin-11	−0.444	0.450	−0.817*	0.167	−0.383	−0.833**
14	A0A5N4DL79	Retinol-binding protein	0.979**	−0.967**	0.083	0.600	0.000	0.467
15	A0A5N4DSC6	Alpha-1B-glycoprotein	0.979**	−0.950**	0.167	0.583	0.100	0.567
16	S9XA78	carboxypeptidase N subunit 2	0.954**	−0.950**	0.067	0.567	−0.050	0.400
17	P68230	Hemoglobin subunit beta	0.979**	−0.950**	0.167	0.583	0.100	0.567
18	S9X3X9	Apolipoprotein D	0.946**	−0.933**	0.050	0.467	0.067	0.433
19	S9XYY2	Hemopexin	0.946**	−0.933**	0.100	0.617	0.000	0.467
20	A0A5N4C6W6	Very-long-chain (3*R*)-3-hydroxyacyl-CoA dehydratase	0.916**	−0.895*	0.184	0.519	0.050	0.485

** $P < 0.01$; * $P < 0.05$.

3.4. Analysis of the expression levels and relative quantitative value of significantly correlated DEPs

The relative quantitative values of 20 DEPs differed significantly in the three muscle groups ($P < 0.05$; Table S1). The relative quantitative values of A0A5N4DTY9 (cadherin - 5), A0A5N4DVE1 (laminin subunit alpha-2), A0A5N4D8E9 (collagen alpha-1 chain), and T0NNA3 (APOBEC-like N-terminal domain-containing protein) were significantly lower in the LT and PM muscles than in the ST muscles ($P < 0.05$). Their levels were higher in the ST muscles than in the LT and PM muscles. Moreover, these proteins were positively correlated with shear force values. The increase in their relative quantitative values increased shear force values, thereby decreasing the tenderness of the ST muscle. However, the relative quantitative values of A0A5N4DL79 (retinol-binding protein) and S9XA78 (carboxypeptidase N subunit 2) were significantly higher in the LT muscles than in the ST and PM muscles ($P < 0.05$). Their levels were higher in the LT muscles than in the ST and PM muscles. Meanwhile, A0A5N4DL79 (retinol-binding protein) and S9XA78 (carboxypeptidase N subunit 2) were significantly higher in the LT muscle than in the ST and PM muscles ($P < 0.05$). Their levels were higher in the LT muscles than in the ST and PM muscles. Meanwhile, A0A5N4DL79 (retinol-binding protein) and S9XA78 (carboxypeptidase N subunit 2) were negatively correlated with shear force values. The increase in their relative quantitative values induced a decrease in shear force values, thereby augmenting the tenderness of the LT and PM muscles compared with the ST muscle. At the same time, the study also revealed that the content of heat shock proteins (HSPs) was positively correlated with the IMF content, whereas negatively correlated with the shear force values. According to the results of data analysis, the content of HSPs was significantly higher in the LT muscles than in the PM and ST muscles. Due to this difference, the IMF content in the LT muscle was relatively higher, while its shear force was relatively lower, in contrast to those observed in the PM and ST muscles. In addition, the results of the correlation analysis revealed a negative correlation between the shear force values and the IMF content values. This fully indicates that the muscles with higher IMF content have lower shear force and thus better tenderness.

3.5. Metabolite profiles of different camel muscles

3.5.1. Identification and classification of metabolites

Changes in the metabolic profiles of muscle samples among the three groups were analyzed using the non-targeted metabolomics method based on UPLC-QE-MS technology. In the superposition analysis of the QC-TIC diagram and sample multi-peak detection diagram (Fig. S4), the metabolome data measured in the present study exhibited good repeatability and reliability. In total, 669 metabolites were identified, including 181 (35.12 %) lipids and lipid-like molecules; 103 (20 %) organic acids and derivatives; 67 (13.01 %) organoheterocyclic compounds; 56 (10.87 %) organic oxygen compounds; 29 (5.63 %) nucleosides, nucleotides, and analogs; 27 (5.24 %) benzenoids; 24 (4.66 %) phenylpropanoids and polyketides; 19 (3.69 %) organic nitrogen compounds; 3 (0.58 %) others; 2 (0.39 %) alkaloids and derivatives; 1 (0.19 %) homogeneous non-metal compound; 1 (0.19 %) hydrocarbon derivative; 1 (0.19 %) hydrocarbon; and 1 (0.19 %) organosulfur compound (Fig. S5).

3.5.2. Multivariate data analysis

The identified metabolite data were analyzed using PCA and PLS-DA methods, and the results are presented in Fig. 4A and Fig. 4B, respectively. Additionally, considering 669 metabolites as independent variables and 3 muscles as dependent variables, the OPLS-DA score chart and validation chart were obtained. The OPLS-DA score plot unveiled (Fig. 4C, E, G) that the sample data of the three groups were located on both sides of the plot. This indicates that this model could effectively distinguish between groups and is suitable for searching for differential metabolites. The prediction parameters R^2Y and Q^2 of the OPLS-DA permutation tests are presented in Fig. 4D, F, and H.

3.5.3. Identification of DEMs

The DEMs were selected based on the OPLS-DA model criteria of VIP > 1 and $P < 0.05$. The PM vs LT, PM vs ST, and LT vs ST groups had 62, 69, and 79 DEMs, respectively. Among the DEMs, 43, 38, and 42 DEMs in the three groups were upregulated, whereas 19, 31, and 37 DEMs were downregulated. Fig. S6A, B, and C present the volcano map analysis of sample data from the PM vs LT, LT vs ST, and PM vs ST groups, respectively. To better visualize these variations, a heatmap was generated by using peak areas of the significant metabolites in the three muscles. As illustrated in Fig. S7A, B, and C, the abundance of 14 metabolites was significantly high in the three muscles, namely L-lsoleucine, *L*-phenylalanine, succinic acid semialdehyde, oxypurinol, vinylacetylglycine, aminoadipic acid, beta-aminobutyric acid L-tryptophan, aspartyl-glutamate, 6-chloro-N-(1-methylethyl)-1,3,5-triazine-2,4-diamine, N2-γ-glutamylglutamine, 2-hydroxyadipic acid, monomenthyl succinate, and 1-cyano-2-hydroxy-3-butene. These DEPs played a vital role in the quality variations of different muscles and can serve as

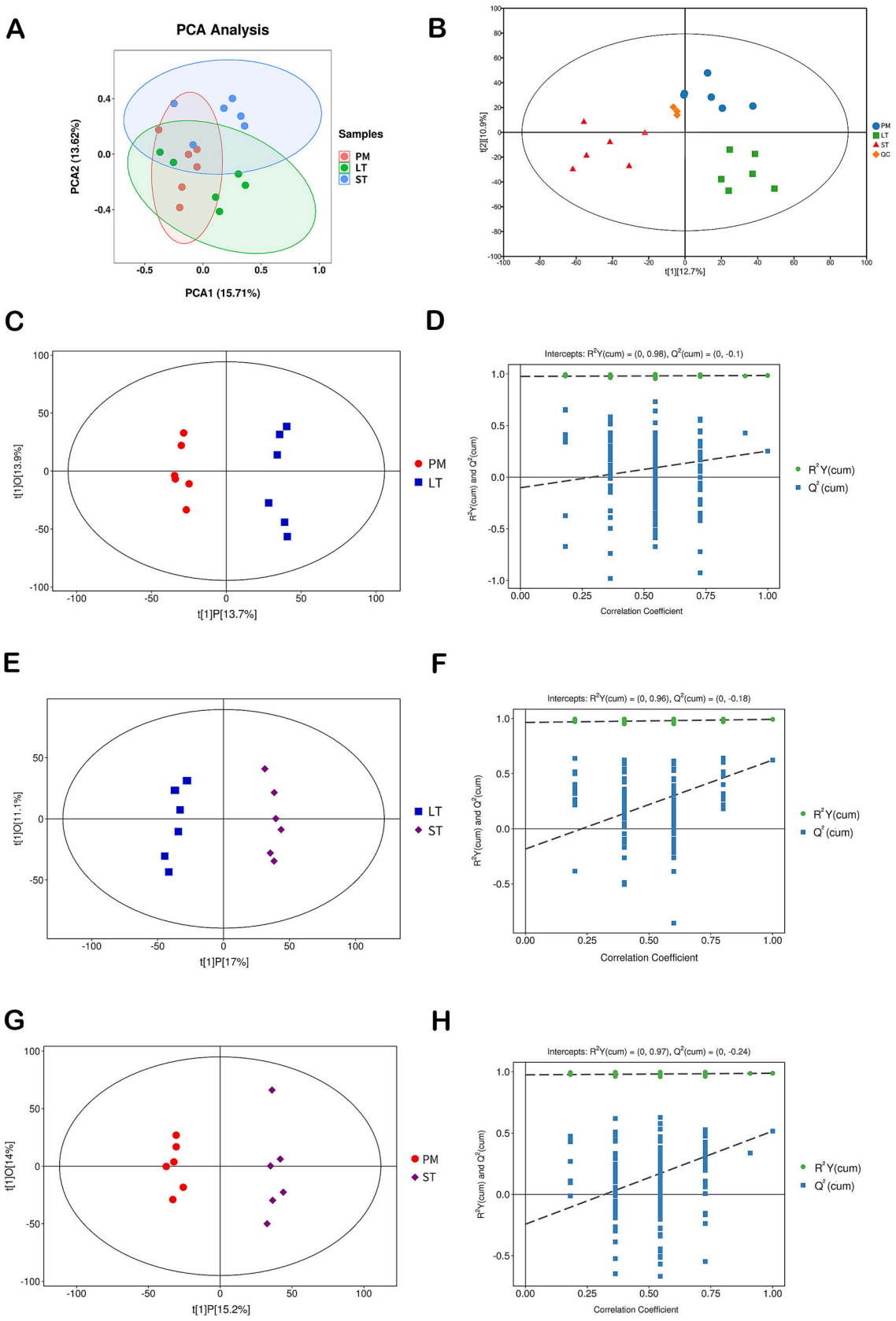

Fig. 4. Results of multivariate data analysis of the three muscles.
(A) PCA model score plots, **(B)** PLS-DA model score plots, **(C, E, and G)** OPLS-DA model score plots, and **(D, F, and H)** permutation test plots. The abbreviations LT, PM, and ST represent longissimus thoracic, psoas major, and semitendinosus, respectively.

a biomarker of metabolites.

3.5.4. KEGG enrichment analysis

The differential metabolites were submitted to the KEGG website for the enrichment analysis of relevant pathways. The top 15 significant pathways were selected to plot KEGG enrichment maps and differential abundance score (DA score) maps. In the PM vs LT group, these DEPs were chiefly involved in carbon metabolism, amino acid biosynthesis, the pentose phosphate pathway, and glycolysis (Fig. 5A). Meanwhile, these metabolic pathways were upregulated in the PM muscle (Fig. 5B). In the LT vs ST group, DEMs were primarily enriched in D-amino acid metabolism, ABC transporters, and glycerophospholipid metabolism (Fig. 5C). Differential metabolic pathways were upregulated in the LT group (Fig. 5D). In the PM vs ST group, DEMs were involved in pathways related to amino acid biosynthesis, protein digestion and absorption, and glycerophospholipid metabolism (Fig. 5E). Except for the glycerophospholipid metabolism pathway, all other pathways were upregulated in the PM muscle (Fig. 5F).

3.6. Analysis of correlation between meat quality indicators and DEMs

Based on the correlation analysis of the relative quantitative values of 20 DEMs and meat quality indicators, 13, 20, 3 and 1 DEPs were significantly associated with the IMF, shear force, L^* value, and pH of meat, respectively (Table S2). Among them, *L*-phenylalanine and PC (18:3(6Z,9Z,12Z)/18:1(11Z)) were extremely significantly correlated with the IMF content ($r = 0.928$, -0.928; $P < 0.01$). *L*-phenylalanine, vinylacetylglycine, aminoadipic acid, and danazol were extremely significantly correlated with shear force ($r = -1$, -1, -1, -1, and 1, respectively; $P < 0.01$). In addition, a significant correlation was observed between the DEMs of *L*-phenylalanine, 3-phosphoglyceric acid, and protopinev and L^* ($r = 0.943$, 0.886, -0.943; $P < 0.05$). One DEM, namely phosphoenolpyruvic acid, was significantly correlated with the pH value ($r = -0.943$; $P < 0.05$). In addition, both the shear force values and the IMF content values had an opposite correlation with the DEMs. This is consistent with the results of the correlation analysis between DEPs and aforementioned quality indicators.

3.7. Analysis of the expression levels and relative quantitative value of significantly correlated DEMs

The relative quantitative value of 20 DEMs differed significantly in the three muscle groups ($P < 0.05$; Table S3). The relative quantitative values of alpha-D-glucose, phosphoenolpyruvic acid, PC (16:0/15:0), protopine, and PC (20:2(11Z,14Z)/14:0) were significantly lower in the LT muscles than in the PM and ST muscles ($P < 0.05$). The relative quantitative values were downregulated in the LT muscle compared with the PM and ST muscles. Moreover, these DEMs were positively correlated with shear force values. The downregulation of relative quantitative values of these DEMs reduced the shear force values, thereby improving the tenderness of the LT muscle. However, the relative quantitative values of adenosine 5′-diphosphate, uridine 5′-diphosphate (UDP), vinylacetylglycine, and thiamine monophosphate were significantly higher in the LT muscles than in the ST and PM muscles ($P < 0.05$). The relative quantitative values were upregulated in the LT muscles compared with the ST and PM muscles. Meanwhile, these DEMs were negatively correlated with shear force values. The upregulation of relative quantitative values of these DEMs induced a decrease in shear force values, thereby augmenting the tenderness of the LT and PM muscles compared with the ST muscle. In addition, the relative quantitative values of protopine, PC(20:2(11Z,14Z)/14:0) and PC(22:2(13Z,16Z)/14:1(9Z)) were significantly higher in the ST muscles than in the LT and PM muscles ($P < 0.05$). Moreover, the afoerementioned three DEMs were negatively correlated with the IMF content of muscle. This may also be the possible reason for the significant differences in IMF content among the three muscles.

3.8. Proteome–metabolome data co-analysis

To determine the association between the results of the proteomic and metabolomic analyses, by choosing metabolic pathways as the carrier, we conducted a mapping analysis based on the differences in proteins and metabolites. Cytoscape software was used to obtain significantly correlated DEPs and DEMs according to the results of Pearson correlation analysis with coefficient values $|\text{cor}| > 0.85$ and $P < 0.05$. We then created a protein–metabolite interaction network diagram. The correlation network of the PM vs LT group had 90 DEPs and 8 DEMs connected by 720 correlations (Fig. S8A). In the LT vs ST group, 35 DEPs and 5 DEMs were connected by 175 correlations (Fig. S8B). The PM vs ST group had 157 DEPs and 31 DEMs connected by 688 correlations (Fig. S8C).

The KEGG pathways, in which DEPs and DEMs were involved, are presented in Fig. 6A, B, and C, respectively. In the PM vs LT group, DEPs and DEMs related to 19 metabolic pathways exhibited changes. The results revealed that pathways such as oxidative phosphorylation, carbon metabolism, amino acid biosynthesis, and the citrate cycle (TCA cycle) were significantly expressed in the PM and LT muscles. In the LT vs ST group, DEPs and DEMs related to 15 metabolic pathways displayed changes. Of them, amino acid biosynthesis, protein digestion and absorption, and carbon metabolism pathways significantly affected the differences between the two muscles. In the PM vs ST group, DEPs and DEMs related to 13 metabolic pathways presented significant changes, chiefly including pathways related to amino acid biosynthesis, glycolysis/gluconeogenesis, and protein digestion and absorption metabolism.

The differential metabolic pathways involving glycolysis/gluconeogenesis, oxidative phosphorylation, amino acid biosynthesis, the citrate cycle (TCA cycle), and carbon metabolism are considered as potential targets for studying the mechanism underlying meat quality in different muscles from bactrian camels. We further investigated differentially enriched proteins and metabolites in meat quality-related metabolic pathways, including amino acid biosynthesis, glycolysis/gluconeogenesis, and the TCA cycle.

Following annotation, glycolysis/gluconeogenesis was sequentially mapped to metabolic pathways (Fig. 6D). The proteins and metabolites with differential abundance were mapped primarily to the glycolysis/gluconeogenesis pathway in KEGG. These proteins and metabolites were quite active between the PM and ST groups. Among them, phosphoglycerate kinase 1 (PGK1) [105095559], fructose bisphosphate A (ALDOA) [105102764], phosphofructokinase muscle (PFKM) [105103800], glyceraldehyde-3-phosphate dehydrogenase (GAPDH) [105098219], enolase 3 (ENO3) [105104769], phosphoglucomutase 1 (PGM1) [105107132], triosephosphate isomerase 1 (TPI1) [105098245], phosphoglycerate mutase 2 (PGAM2) [105103438], fructose-bisphosphate C (ALDOC) [105088182], enolase 2 (ENO2) [105098197], phosphoglycerate kinase 2 (PGK2) [105096574], and phosphoenolpyruvate were upregulated. As seen in Fig. 6E, in the LT vs ST group, aspartate aminotransferase [105084303] and alanine aminotransferase 2 [105091190] were downregulated in the alanine, aspartate, and glutamate metabolism, whereas L-glutamine was upregulated. The citrate cycle (TCA cycle) metabolic pathway was enriched in 7 DEPs and 1 DEM (Fig. 6F). Of them, aconitase 2 (ACO2) [105091900], MDH2 [105089651], isocitrate dehydrogenase (NADP (+)) 2 (IDH2) [105094685], FH [105099273], SDHB [105107079], SDHB [105107079], DLST [105086098], isocitrate dehydrogenase (NAD (+)) 3 catalytic subunit alpha (IDH3A) [105092226], and phosphoenolpyruvate were upregulated.

4. Discussion

Muscle type is a significant factor influencing the quality traits of meat, and knowledge about the quality of meat from different muscles is essential for developing the camel meat market (Kadim et al., 2013; Si, Na, et al., 2022). Although camel meat quality has been extensively

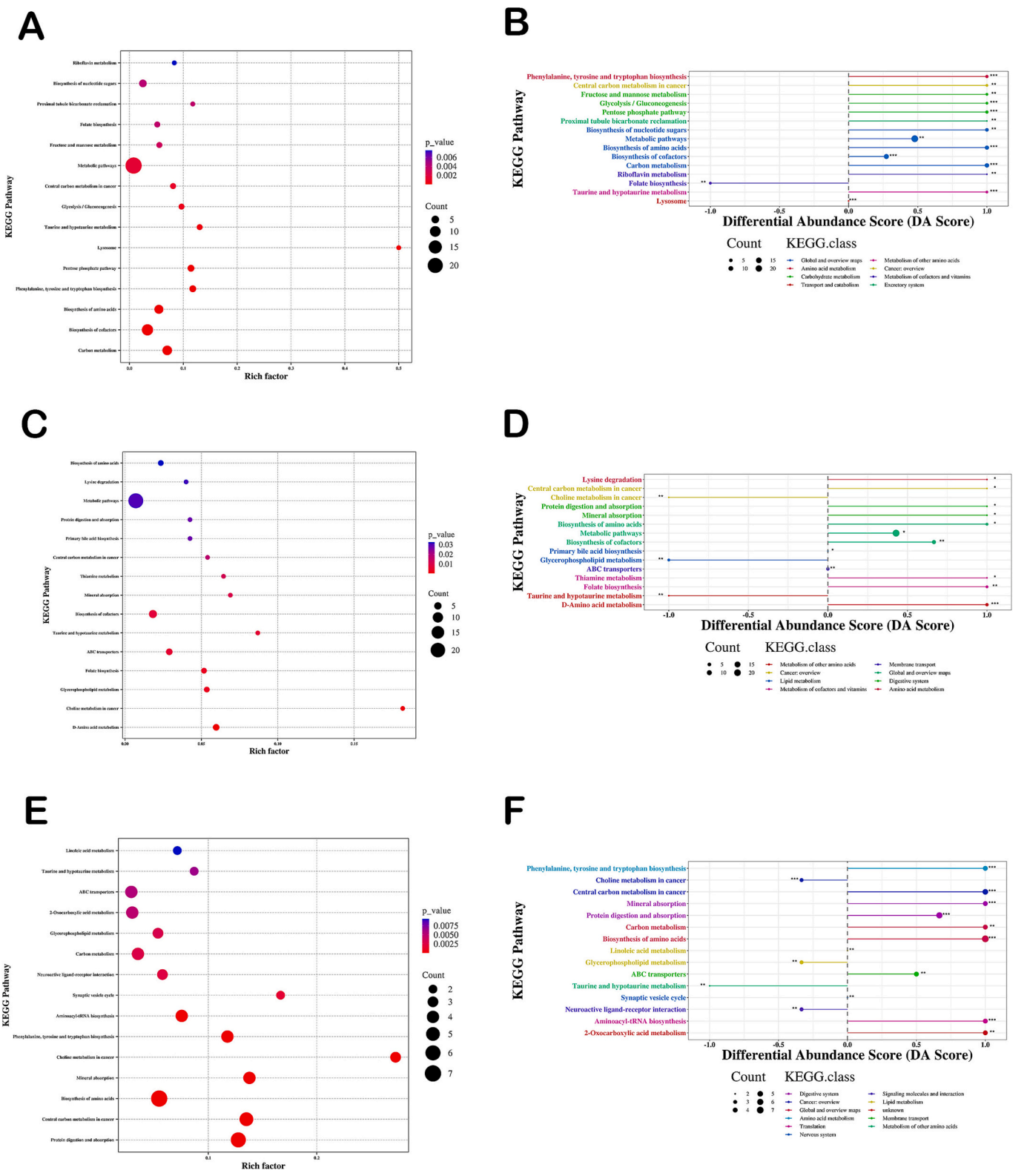

Fig. 5. Metabolic pathway enrichment map and DA scores of DEMs from the three muscles.
A, **C,** and **E** represent the top 15 metabolic pathways enriched in the PM vs LT, LT vs ST, and PM vs ST groups, respectively. **B**, **D,** and **F** represent the DA scores for the PM vs LT, LT vs ST, and PM vs ST groups, respectively. The abbreviations LT, PM, and ST denote longissimus thoracic, psoas major, and semitendinosus, respectively. The larger the graph, the more the number of DEMs. The color indicates the significance of enrichment, that is, the *P* value. A darker red color indicates that the pathway is more significantly enriched. (For interpretation of the references to color in this figure legend, the reader is referred to the web version of this article.)

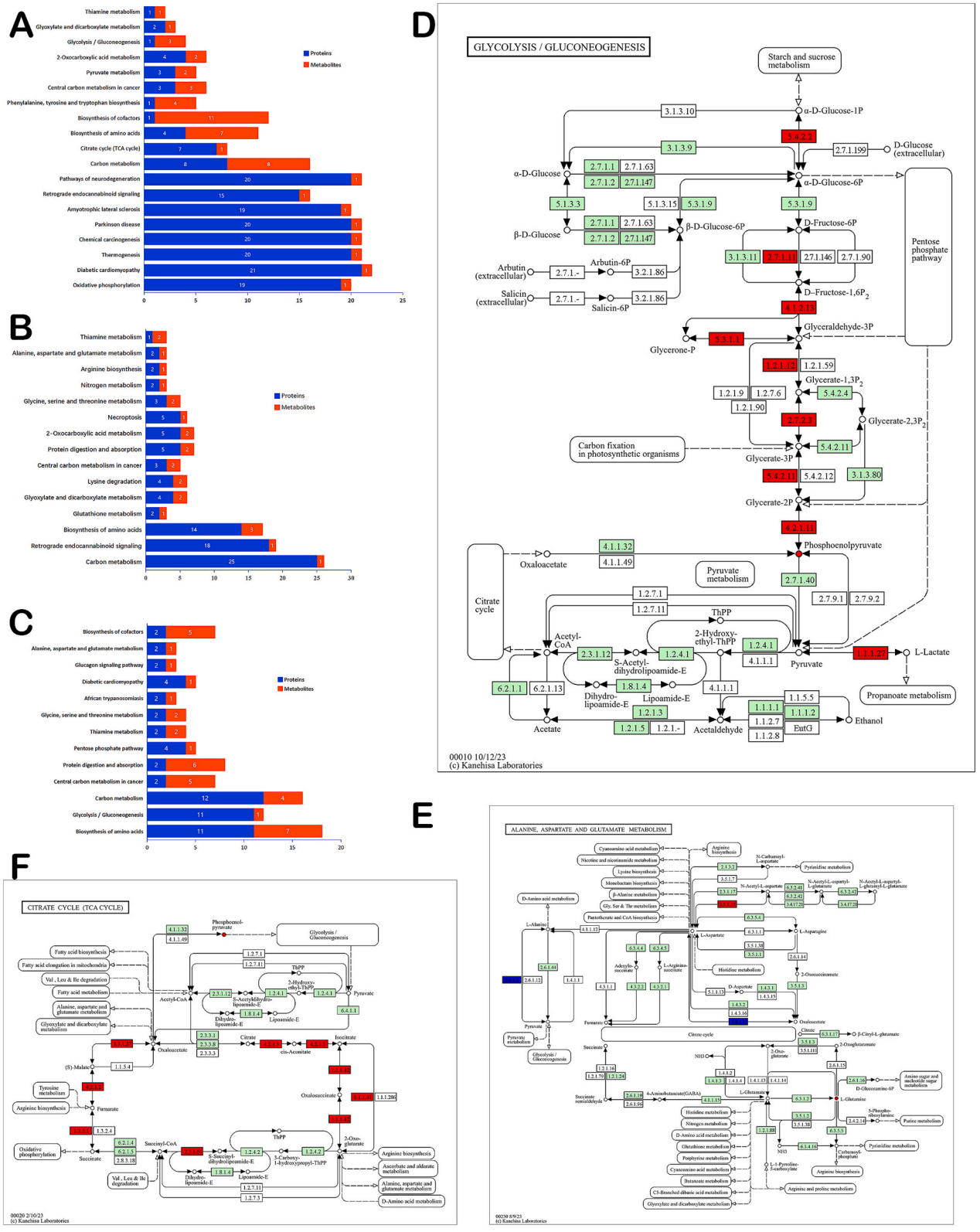

Fig. 6. Metabolic pathway coenriched by DEPs and DEMs.
A, **B,** and **C** represent the common pathways of candidate proteins and metabolites. The signaling pathways of proteins and metabolites commonly involved in longissimus thoracic, psoas major, and semitendinosus from camels. Blue represents the number of DEPs. Red represents the number of DEMs.
(D) Glycolysis/gluconeogenesis pathway; **(E)** alanine, aspartate, and glutamate metabolism; and **(F)** citrate cycle (TCA cycle) metabolic pathway. Proteins (□) and metabolites (o) with differential abundance, which were involved in metabolism pathways, were mapped to the corresponding metabolic pathways in KEGG. Red indicates upregulation, whereas blue indicates downregulation. (For interpretation of the references to color in this figure legend, the reader is referred to the web version of this article.)

studied for many years, a comprehensive study investigating metabolites, proteins, and key regulatory pathways related to different muscles from camel meat by using multi-omics is lacking. Yu, Tian, et al. (2023) determined the relationship between IMF content and meat quality in pork by using transcriptome, proteome, and metabolomics techniques, thus providing insights into fat deposition and meat quality in pigs. By performing an integrated multiomic analysis, Yu, Wang, et al. (2023) investigated the variation in IMF content between different muscle locations of Qinchuan cattle. Huang et al.'s (2020) recent study provided further anchorage to the current study; in that study, the researchers integrated proteomics and metabolomics to discover the potential meat quality indicators of postmortem lamb. These findings reflect the necessity to address the integration of proteomics and metabolomics in the present study. Therefore, we here conducted proteomic and metabolomic studies of different camel muscles and obtained corresponding DEPs and DEMs. Accordingly, an integrated analysis of the metabolic pathways associated with these DEPs and DEMs was conducted to explain the impact of these DEPs and DEMs on the quality of camel meat and to unveil the molecular mechanisms underlying the differences in the quality of meat from different camel muscles.

4.1. Proteomic profiles of different camel muscles

Different muscles exert substantial effects on meat quality characteristics (Kadim et al., 2013; Si, Na, et al., 2022). Therein, the meat protein composition and content exert considerable effects on meat color, tenderness, and myofibrillar ultrastructure (Zhou et al., 2021). In particular, proteins such as troponint, myosin heavy chain, and myosin light chain are known to be closely associated with meat quality (Mora et al., 2010). Meanwhile, the identified DEPs also involved numerous structural proteins. In the present study, significant differences in cytoskeleton-related proteins, such as myosin, calcium-binding protein, α-tubulin, titin, collagen alpha-1 chain, calcium-regulated heat stable protein 1, and tropomyosin, were observed among the three muscles. Moreover, the DEPs identified in the three muscles involved numerous metabolic enzymes and stress proteins such as GAPDH, NADH dehydrogenase, pyruvate kinase, and HSPs. GAPDH is a vital enzyme participating in the glycolytic pathway. It promotes aldehyde oxidation and phosphorylation to generate acyl phosphates, thereby producing ATP through the electron transfer chain (Mahmood et al., 2018). It affects muscle quality characteristics through the carbohydrate metabolism pathway and significantly influences quality indicators such as cooking loss, color, and tenderness of muscles. Additionally, actin is significantly associated with muscle color (a^* and b^* values), shear force, cooking loss, and pH values (Li et al., 2017). In preset study, in the LT vs ST group, the expression of Xin actin-binding repeat-containing protein 1 (XIRP1) was upregulated (3.6 FC). By contrast, in the PM vs LT group, XIRP1 expression was downregulated (0.45 FC), indicating a higher XIRP1 protein content in the LT muscle. This may have resulted in quality differences in the meat from the LT muscle compared with the other muscles.

Pyruvate kinase (PK) is among the key rate-limiting enzymes in glycolysis. It catalyzes the transfer of energy from phosphoenolpyruvate to ADP, thereby producing pyruvate and ATP. In this study, PK was upregulated in both the LT vs ST and PM vs ST groups, and its content may affect the meat's pH value. NADH dehydrogenase was also among the most significantly expressed proteins in the three muscles. According to Xin et al. (2018), NADH dehydrogenase was overexpressed in dark pork because of its increased oxidative metabolism. This indicates that NADH dehydrogenase is a major protein causing color differences in LT, PM, and ST muscles in this study.

HSPs, also known as stress proteins, are members of the companion family of proteins. These proteins are induced under high temperature, hypoxia, and other stress conditions and can prevent denaturation and aggregation of postmortem meat proteins (Lee & Choi, 2021). Zhang et al. (2023) reported that stress proteins can serve as potential biomarkers of changes in the post-slaughter muscle myofibrillar structure. In this study, HSP beta-2, HSP beta-3, and HSP22 are upregulated in the LT vs ST and PM vs ST groups, whereas they were downregulated in the PM vs LT group. This relative change in content was basically consistent with the previously discussed difference in changes in the shear force values of the three muscles, which suggests that HSPs have a rather greater impact on meat tenderness. Similar findings have also been reported in other studies (Cui et al., 2018; Ding et al., 2022).

Collagen is a major structural protein in muscles. Its differential expression can directly affect the mechanical properties of the muscles. A higher collagen content may lead to an increase in cross-linking within muscle fibers, making the meat tougher and thus increasing the shear force required to cut it (Kadim et al., 2006). In this study, this phenomenon comprehensively illustrates that the relatively elevated collagen content within the ST muscles constitutes the primary factor accounting for their greater shear force than that of the LT and PM muscles (Table S1).

Through the KEGG enrichment analysis, we found that glycolytic metabolism, oxidative phosphorylation, the citrate cycle (TCA cycle), and amino acid biosynthesis can be considered as potential targets for studying the mechanism underlying changes in the meat quality of different muscles. The glycolytic metabolic pathway is among the major pathways associated with meat quality. It affects changes in muscle pH, which directly or indirectly regulates quality indicators such as water-holding capacity, tenderness, and color (Chen et al., 2019; Wei et al., 2019). In the PM vs ST group, glycolysis was most significantly enriched, with 12 upregulated DEPs (namely GAPDH, aldolase, ALDOA, ENO3, L-lactate dehydrogenase A chain (LOC105095329), TPI1, PGK1, PFKM, PGM1, PGAM2, ALDOC, and PGK2). This can explain why the pH value of the ST muscle (6.11) was significantly higher ($P < 0.05$) than that of the PM muscle (5.58).

4.2. Metabolite profiles of different camel muscles

We used metabolomics to analyze the metabolic profiles of meat from three muscles and screened for differential metabolites. A total of 14 differential metabolites and the metabolic pathways they are enriched in were observed. These metabolites and their pathways might be the primary reasons for the differences in meat quality. The KEGG enrichment analysis unveiled significant differences in carbon metabolism, amino acid biosynthesis, the pentose phosphate pathway, and glycolysis metabolism in the PM vs LT group. The aforementioned pathways were all upregulated in the PM muscle. Metabolites such as dihydroxyacetone phosphate, D-ribose-5-phosphate, D-ribulose 5-phosphate, *L*-phenylalanine, and phosphoenolpyruvate participated in metabolic pathways such as carbon metabolism, amino acid metabolism, and the pentose phosphate pathway. The expression of these metabolites was upregulated and their concentrations were increased. This indicated that the PM muscle promotes nutrient digestion and metabolism and boosts muscle growth and development. In energy metabolism, glycolysis and the TCA cycle are the key pathways providing energy (Antonelo et al., 2022). The upregulated metabolites in the present study, such as dihydroxyacetone phosphate, alpha-D glucose, and phosphoenolpyruvate, are involved in the glycolysis metabolic pathway. Pyruvate is a key metabolite in glycolysis and the TCA cycle, and its increased concentration can promote energy metabolism (Nelson & Cox, 2007). The muscle glycolysis activity is related to meat tenderness and pH (Wu, 2015). In this study, metabolites such as *L*-phenylalanine, *D*-erythrise-4-phosphate, phosphoenolpyruvate, and *L*-tryptophan were upregulated in the biosynthetic metabolic pathways of phenylalanine, tyrosine, and tryptophan, thereby significantly improving the flavor characteristics of camel meat. The study proves that the increase in *L*-tryptophan content can effectively solve the problem of pre-slaughter stress-induced pale soft exudative of meat (Yang et al., 2022).

In the LT vs ST group, metabolic pathways, such as D-amino acid

metabolism, ABC transporters, glycerophospholipid metabolism, and taurine and hypotaurine metabolism, were significantly enriched. Except for the glycerophospholipid metabolism pathway, all other pathways were upregulated in the LT group. L-glutamine and glycine were upregulated in D-amino acid metabolism and ABC transporter metabolic pathways. D-amino acids possess remarkable antioxidant and antibacterial effects (Lee et al., 2022), which considerably influence the flavor and quality of food. Taurine is also an amino acid with a crucial role in neurodevelopment, endocrine function, immune function, and lipid absorption (Wu, 2009). In the present study, taurine was primarily involved in taurine and hypotaurine metabolism, neuroactive ligand–receptor interaction, primary bile acid biosynthesis, ABC transporters, and sulfur metabolism. The results indicated that the taurine content was significantly higher in the ST muscle than in the PM and LT muscles. Moreover, the present study found that the eicosapentaenoic acid content was the highest in the ST muscle, followed by the PM and LT muscles. Simultaneously, eicosapentaenoic acid was significantly enriched in the biosynthetic metabolic pathway of unsaturated fatty acids. This reflected that the eicosapentaenoic acid content significantly increased the content of polyunsaturated fatty acids and n-6/n-3, and the UFA/SFA ratio in the muscles. This result was consistent with the author's previous findings that the unsaturated fatty acid content was significantly higher in the ST muscle than in the PM and LT muscles (Si, Na, et al., 2022).

4.3. Proteome–metabolome data co-analysis

Through the integrated analysis of proteomic and metabolomic data from three muscles, 282 DEPs and 44 DEMs exhibiting correlation were identified. This indicated that the combined effect of these proteins and metabolites was closely related to the nutritional composition of meat and changes in meat quality. These proteins predominantly included nebulin, HSPs, 3-hydroxyisobutyrate dehydrogenase, NADH dehydrogenase, etc. Meanwhile, the identified metabolites primarily included 3-phosphoglyceraldehyde dehydrogenase, *L*-phenylalanine, *L*-tryptophan, taurine, *L*-tyrosine, etc. Structural proteins such as nebulin and HSPs have a significant effect on the muscle fiber structure (*Z*-band, I-band) of fresh meat and thus influence muscle tenderness (Ming & Shiwei, 2020). Additionally, metabolites such as *L*-phenylalanine, *L*-tryptophan, and L-serine are of marked significance for muscle growth and development, quality characteristics, and energy metabolism (Deng et al., 2023).

The meat quality characteristics (such as tenderness, color, and juiciness) are critical factors that consumers consider when purchasing meat. Energy metabolism in muscles significantly influences the growth, development, and maturation of muscles, thereby affecting meat quality. The phosphocreatine system, glycolytic pathways, and oxidative phosphorylation are the key ATP sources for muscles and play a crucial role in determining muscle quality (Huang et al., 2023). In this study, DEPs (ATP synthase subunit alpha, NADH-ubiquinone oxidoreductase, succinate dehydrogenase, acyl carrier protein, etc.) and the DEM (adenosine diphosphate) were together involved in the oxidative phosphorylation metabolic pathway. In living organisms, ATP synthase is the key enzyme for energy synthesis and is widely distributed in various tissues and cells. Being an important component of the mitochondrial oxidative phosphorylation system, this enzyme primarily plays a role in ATP synthesis or hydrolysis within cells or cell membranes (Cheuk & Meier, 2021). Additionally, glycolysis and the TCA cycle are crucial energy metabolism pathways in animal meat. In addition, DEPs such as aconitate hydratase, malate dehydrogenase, isocitrate dehydrogenase, fumarate hydratase, and succinate dehydrogenase and the DEM phosphoenolpyruvate were coenriched in the TCA cycle metabolic pathway. The aconitic acid enzyme is a key enzyme of the TCA cycle. Upregulation of this enzyme increases the aconitic acid concentration in the TCA cycle, thus effectively promoting energy metabolism (Nelson & Cox, 2007). The muscle glycolytic activity and the pentose phosphate pathway are related to meat tenderness and the pH value (Yun, 2015). DEPs, such as aldolase, ALDOA, PFKM, and PGM1, and DEMs such as D-erythrise-4-phosphate and phosphoenolpyruvate were significantly enriched in the aforementioned two pathways. We inferred that these differential proteins and metabolites, as well as their coenriched metabolic pathways, played a crucial role in the differences in the shear force and pH value of the three muscles.

Therefore, the integrated proteomic and metabolomic analysis unveiled that the DEP- and DEM-enriched metabolic pathways were closely related to meat quality. Significant differences in these metabolic pathways may serve as intrinsic factors causing variations in the quality characteristics of LT, PM, and ST muscles.

5. Conclusion

This is the first study that detects the profiles of proteins and metabolites in the camel meat from different muscles. The determination of that meat quality indicators revealed IMF, shear force, pH, and L^* values varied significantly among different muscles. LT muscles had higher IMF content, which were also tender and had a lower shear force value than ST and PM muscles. Furthermore, the crucial proteins, metabolites, and metabolic pathways that affect these quality changes were emphatically analyzed. In total, 552 DEPs were identified in the three muscles. The PM vs LT, PM vs ST, and LT vs ST comparison groups had 141, 196, and 436 DEPs, respectively. Functional analysis demonstrated that collagen, HSPs, myosin, retinol-binding protein, and cadherin-5 could act as crucial proteins for distinct muscles. Simultaneously, the relative quantitative values of these proteins exhibited a significant correlation with the shear force values and IMF contents. Metabolome analysis revealed that the PM vs LT, LT vs ST, and PM vs ST comparison groups had 62, 79, and 69 DEMs, respectively. Among them, phosphoenolpyruvic acid, *L*-phenylalanine, PC(20:2(11Z,14Z)/14:0), and PC(22:2(13Z,16Z)/14:1(9Z)) were key factors contributing to the quality variations in meat from different muscles. The co-analysis of proteomics and metabolomics revealed that the differential metabolic pathways involving glycolysis, oxidative phosphorylation and the citrate cycle (TCA cycle) were considered as potential targets for studying the mechanism underlying meat quality of different muscles from bactrian camels. These findings provide valuable evidence of the proteins and metabolites that regulate meat quality, offering important insights into the mechanisms underlying the development of superior meat products. Future studies are need for a functional validation of identified proteins and metabolites to establish a causal relationship between pathway regulation and meat quality.

Funding information

This research was supported by the the Research Fund of First-class Disciplines (grant number YLXKZX-NND-017), the National Key Research and Development Project (grant number 2020YFE0203300) and the Inner Mongolia Autonomous Region Science and Technology Plan Project (grant number 2019GG359).

CRediT authorship contribution statement

Rendalai Si: Writing – review & editing, Writing – original draft, Visualization, Methodology, Investigation, Formal analysis. **Liang Ming:** Writing – original draft, Investigation. **Xueyan Yun:** Writing – review & editing. **Jing He:** Investigation, Formal analysis. **Li Yi:** Visualization. **Qin Na:** Validation, Software. **Rimutu Ji:** Project administration, Methodology, Funding acquisition, Conceptualization. **Tungalag Dong:** Writing – review & editing, Supervision, Project administration, Conceptualization.

Declaration of competing interest

The authors declare that they have no known competing financial

interests or personal relationships that could have appeared to influence the work reported in this paper.

Appendix A. Supplementary data

Supplementary data to this article can be found online at https://doi.org/10.1016/j.fochx.2025.102230.

Data availability

Data will be made available on request.

References

Al-Owaimer, A. N., Suliman, G. M., Sami, A. S., Picard, B., & Hocquette, J. F. (2014). Chemical composition and structural characteristics of Arabian camel (Camelus dromedarius) m. longissimus thoracis. *Meat Science, 96*, 1233–1241. https://doi.org/10.1016/j.meatsci.2013.10.025

Antonelo, D. S., Dos Santos-Donado, P. R., Ferreira, C. R., Colnago, L. A., Ocampos, F. M. M., Ribeiro, G. H., … Balieiro, J. C. C. (2022). Exploratory lipidome and metabolome profiling contributes to understanding differences in high and normal ultimate pH beef. *Meat Science, 194*, Article 108978. https://doi.org/10.1016/j.meatsci.2022.108978

Baba, W. N., Rasool, N., Selvamuthukumara, M., & Maqsood, S. (2021). A review on nutritional composition, health benefits, and technological interventions for improving consumer acceptability of camel meat: An ethnic food of Middle East. *Journal of Ethnic Foods, 8*, 18. https://doi.org/10.1186/s42779-021-00089-1

Biffin, T. E., Smith, M. A., Bush, R. D., Morris, S., & Hopkins, D. L. (2020). The effect of whole carcase medium voltage electrical stimulation, tenderstretching and longissimus infusion with actinidin on alpaca meat quality. *Meat Science, 164*, Article 108107. https://doi.org/10.1016/j.meatsci.2020.108107

Burger, P. A., Ciani, E., & Faye, B. (2019). Old World camels in a modern world - a balancing act between conservation and genetic improvement. *Animal Genetics, 50*, 598–612. https://doi.org/10.1111/age.12858

Chatterjee, N. S., Chevallier, O. P., Wielogorska, E., Black, C., & Elliott, C. T. (2019). Simultaneous authentication of species identity and geographical origin of shrimps: Untargeted metabolomics to recurrent biomarker ions. *Journal of Chromatography A, 1599*, 75–84. https://doi.org/10.1016/j.chroma.2019.04.001

Chen, L., Li, Z., Everaert, N., Lametsch, R., & Zhang, D. (2019). Quantitative phosphoproteomic analysis of ovine muscle with different postmortem glycolytic rates. *Food Chemistry, 280*, 203–209. https://doi.org/10.1016/j.foodchem.2018.12.056

Cheng, H., Song, S., Jung, E. Y., Jeong, J. Y., Joo, S. T., & Kim, G. D. (2020). Comparison of beef quality influenced by freeze-thawing among different beef cuts having different muscle fiber characteristics. *Meat Science, 169*, Article 108206. https://doi.org/10.1016/j.meatsci.2020.108206

Cheuk, A., & Meier, T. (2021). Rotor subunits adaptations in ATP synthases from photosynthetic organisms. *Biochemical Society Transactions, 49*, 541–550. https://doi.org/10.1042/bst20190936

Cui, Y., Hao, Y., Li, J., Gao, Y., & Gu, X. (2018). Proteomic changes of the porcine skeletal muscle in response to chronic heat stress. *Journal of the Science of Food and Agriculture, 98*, 3315–3323. https://doi.org/10.1002/jsfa.8835

Deng, L., Li, W., Liu, W., Liu, Y., Xie, B., Groenen, M. A. M., … Tang, Z. (2023). Integrative metabolomic and transcriptomic analysis reveals difference in glucose and lipid metabolism in the longissimus muscle of Luchuan and Duroc pigs. *Frontiers in Genetics, 14*, 1128033. https://doi.org/10.3389/fgene.2023.1128033

Ding, Z., Wei, Q., Liu, C., Zhang, H., & Huang, F. (2022). The quality changes and proteomic analysis of cattle muscle postmortem during rigor mortis. *Foods, 11*, 217. https://doi.org/10.3390/foods11020217

Dunn, W. B., Broadhurst, D., Begley, P., Zelena, E., Francis-McIntyre, S., Anderson, N., … Goodacre, R. (2011). Procedures for large-scale metabolic profiling of serum and plasma using gas chromatography and liquid chromatography coupled to mass spectrometry. *Nature Protocols, 6*, 1060–1083. https://doi.org/10.1038/nprot.2011.335

Fan, W., Ge, G., Liu, Y., Wang, W., Liu, L., & Jia, Y. (2018). Proteomics integrated with metabolomics: Analysis of the internal causes of nutrient changes in alfalfa at different growth stages. *BMC Plant Biology, 18*(1), 78. https://doi.org/10.1186/s12870-018-1291-8

Hou, X., Liu, Q., Meng, Q., Wang, L., Yan, H., Zhang, L., & Wang, L. (2020). TMT-based quantitative proteomic analysis of porcine muscle associated with postmortem meat quality. *Food Chemistry, 328*, Article 127133. https://doi.org/10.1016/j.foodchem.2020.127133

Huang, C., Blecker, C., Chen, L., Xiang, C., Zheng, X., Wang, Z., & Zhang, D. (2023). Integrating identification and targeted proteomics to discover the potential indicators of postmortem lamb meat quality. *Meat Science, 199*, Article 109126. https://doi.org/10.1016/j.meatsci.2023.109126

Huang, C., Hou, C., Ijaz, M., Yan, T., Li, X., Li, Y., & Zhang, D. (2020). Proteomics discovery of protein biomarkers linked to meat quality traits in post-mortem muscles: Current trends and future prospects: A review. *Trends in Food Science & Technology, 105*, 416–432. https://doi.org/10.1016/j.tifs.2020.09.030

Hwang, Y. H., Lee, E. Y., Lim, H. T., & Joo, S. T. (2023). Multi-omics approaches to improve meat quality and taste characteristics. *Food Science of Animal Resources, 43*, 1067–1086. https://doi.org/10.5851/kosfa.2023.e63

Kadim, I. T., Al-Amri, I. S., Alkindi, A. Y., & Haq, Q. M. I. (2022). Nutritional values and health benefits of dromedary camel meat. *Animal Frontiers, 12*, 61–70. https://doi.org/10.1093/af/vfac051

Kadim, I. T., Al-Amri, I. S., Kindi, A. Y. A., & Mbaga, M. D. (2018). Camel meat production and quality: A review. *Journal of Camel Practice and Research, 25*, 9–23.

Kadim, I. T., Al-Karousi, A., Mahgoub, O., Al-Marzooqi, W., Khalaf, S. K., Al-Maqbali, R. S., … Raiymbek, G. (2013). Chemical composition, quality and histochemical characteristics of individual dromedary camel (Camelus dromedarius) muscles. *Meat Science, 93*, 564–571. https://doi.org/10.1016/j.meatsci.2012.11.028

Kadim, I. T., Mahgoub, O., Al-Marzooqi, W., Al-Zadjali, S., Annamalai, K., & Mansour, M. H. (2006). Effects of age on composition and quality of muscle longissimus thoracis of the Omani Arabian camel (Camelus dromedaries). *Meat Science, 73*, 619–625. https://doi.org/10.1016/j.meatsci.2006.03.002

Kadim, I. T., Mahgoub, O., & Purchas, R. W. (2008). A review of the growth, and of the carcass and meat quality characteristics of the one-humped camel (Camelus dromedaries). *Meat Science, 80*, 555–569. https://doi.org/10.1016/j.meatsci.2008.02.010

Kurtu, M. Y. (2004). An assessment of the productivity for meat and the carcass yield of camels (Camelus dromedarius) and of the consumption of camel meat in the eastern region of Ethiopia. *Tropical Animal Health and Production, 36*, 65–76. https://doi.org/10.1023/b:trop.0000009520.34657.35

Lee, B., & Choi, Y. M. (2021). Research note: Comparison of histochemical characteristics, chicken meat quality, and heat shock protein expressions between PSE-like condition and white-stripping features of pectoralis major muscle. *Poultry Science, 100*, Article 101260. https://doi.org/10.1016/j.psj.2021.101260

Lee, C. J., Qiu, T. A., Hong, Z., Zhang, Z., Min, Y., Zhang, L., … Sweedler, J. V. (2022). Profiling of d-alanine production by the microbial isolates of rat gut microbiota. *FASEB Journal, 36*, Article e22446. https://doi.org/10.1096/fj.202101595R

Li, S., Tian, Y., Jiang, P., Lin, Y., Liu, X., & Yang, H. (2021). Recent advances in the application of metabolomics for food safety control and food quality analyses. *Critical Reviews in Food Science and Nutrition, 61*, 1448–1469. https://doi.org/10.1080/10408398.2020.1761287

Li, Z., Li, X., Gao, X., Shen, Q. W., Du, M., & Zhang, D. (2017). Phosphorylation prevents in vitro myofibrillar proteins degradation by μ-calpain. *Food Chemistry, 218*, 455–462. https://doi.org/10.1016/j.foodchem.2016.09.048

Liu, H., Wei, B., Tang, Q., Chen, C., Li, Y., Yang, Q., Wang, J., Li, J., Qi, J., Xi, Y., Hu, J., Hu, B., Bai, L., Han, C., Wang, J., & Li, L. (2022). Non-target metabolomics reveals the changes of small molecular substances in duck breast meat under different preservation time. *Food Research International, 161*, Article 111859. https://doi.org/10.1016/j.foodres.2022.111859

López-Pedrouso, M., Lorenzo, J. M., Cittadini, A., Sarries, M. V., Gagaoua, M., & Franco, D. (2023). A proteomic approach to identify biomarkers of foal meat quality: A focus on tenderness, color and intramuscular fat traits. *Food Chemistry, 405*, Article 134805. https://doi.org/10.1016/j.foodchem.2022.134805

Lyu, H., Na, Q., Wang, L., Li, Y., Zheng, Z., Wu, Y., … Ming, L. (2024). Effects of muscle type and aging on glycolysis and physicochemical quality properties of Bactrian camel (Camelus bactrianus) meat. *Animals (Basel), 14*, 611. https://doi.org/10.3390/ani14040611

Mahmood, S., Turchinsky, N., Paradis, F., Dixon, W. T., & Bruce, H. L. (2018). Proteomics of dark cutting longissimus thoracis muscle from heifer and steer carcasses. *Meat Science, 137*, 47–57. https://doi.org/10.1016/j.meatsci.2017.11.014

Ming, Z., & Shiwei, Y. (2020). Function and clinical research progress of actin-associated anchor protein. *Chinese Journal of Cardiology (in Chinese), 03*, 315–318.

Mora, L., Hernández-Cázares, A. S., Aristoy, M. C., & Toldrá, F. (2010). Hydrophilic interaction chromatographic determination of adenosine triphosphate and its metabolites. *Food Chemistry, 123*, 1282–1288. https://doi.org/10.1016/j.foodchem.2010.05.072

Nelson, D. L., & Cox, M. M. (2007). *Lehninger principles of biochemistry*. New York: Freeman and Company.

Rozanova, S., Barkovits, K., Nikolov, M., Schmidt, C., Urlaub, H., & Marcus, K. (2021). Quantitative mass spectrometry-based proteomics: An overview. *Methods in Molecular Biology, 2228*, 85–116. https://doi.org/10.1007/978-1-0716-1024-4_8

Si, R., Na, Q., Wu, D., Wu, X., Ming, L., & Ji, R. (2022). Effects of age and muscle type on the chemical composition and quality characteristics of Bactrian camel (Camelus bactrianus) meat. *Foods, 11*, 1021. https://doi.org/10.3390/foods11071021

Si, R., Wu, D., Na, Q., He, J., Yi, L., Ming, L., … Ji, R. (2022). Effects of various processing methods on the nutritional quality and carcinogenic substances of Bactrian camel (Camelus bactrianus) meat. *Foods, 11*, 3276. https://doi.org/10.3390/foods11203276

Suliman, G. M., Al-Owaimer, A. N., Hussein, E. O. S., Abuelfatah, K., & Othman, M. B. (2020). Meat quality characteristics of the Arabian camel (Camelus dromedarius) at different ages and post-mortem ageing periods. *Asian-Australasian Journal of Animal Sciences, 33*, 1332–1338. https://doi.org/10.5713/ajas.19.0589

Tschirhart-Hoelscher, T. E., Baird, B. E., King, D. A., McKenna, D. R., & Savell, J. W. (2006). Physical, chemical, and histological characteristics of 18 lamb muscles. *Meat Science, 73*, 48–54. https://doi.org/10.1016/j.meatsci.2005.10.015

Wei, Y., Li, X., Zhang, D., & Liu, Y. (2019). Comparison of protein differences between high- and low-quality goat and bovine parts based on iTRAQ technology. *Food Chemistry, 289*, 240–249. https://doi.org/10.1016/j.foodchem.2019.03.052

Wu, G. (2009). Amino acids: Metabolism, functions, and nutrition. *Amino Acids, 37*, 1–17. https://doi.org/10.1007/s00726-009-0269-0

Wu, X. Y. (2015). *Screening and identification of candidate proteins for quality traits of yak meat*. Chinese Academy of Agricultural Sciences. (in Chinese).

Xin, J., Li, Z., Li, X., Li, M., Li, G., Rao, W., & Zhang, D. (2018). Meat color stability of ovine muscles is related to glycolytic dehydrogenase activities. *Journal of Food Science, 83*, 2432–2438. https://doi.org/10.1111/1750-3841.14321

Yang, T., Liu, R., Yang, L., Yang, W., Li, K., Qin, M., … Zhou, X. (2022). Improvement strategies for quality defects and oxidation of pale, soft and exudative (PSE)-like chicken meat: Effects of domestic cooking and core temperature. *RSC Advances, 12*, 7485–7496. https://doi.org/10.1039/d2ra00392a

Yu, H., Wang, J., Zhang, K., Cheng, G., Mei, C., & Zan, L. (2023). Integrated multi-omics analysis reveals variation in intramuscular fat among muscle locations of Qinchuan cattle. *BMC Genomics, 24*, 367. https://doi.org/10.1186/s12864-023-09452-9

Yu, T., Tian, X., Li, D., He, Y., Yang, P., Cheng, Y., Zhao, X., Sun, J., & Yang, G. (2023). Transcriptome, proteome and metabolome analysis provide insights on fat deposition and meat quality in pig. *Food Research International, 166*, Article 112550. https://doi.org/10.1016/j.foodres.2023.112550

Zarrin, M., Riveros, J. L., Ahmadpour, A., de Almeida, A. M., Konuspayeva, G., Vargas-Bello-Pérez, E., … Hernández-Castellano, L. E. (2020). Camelids: New players in the international animal production context. *Tropical Animal Health and Production, 52*, 903–913. https://doi.org/10.1007/s11250-019-02197-2

Zhang, L., Li, Q., Sørensen, J. S., Luo, Y., & Lametsch, R. (2023). Protein phosphorylation profile of Atlantic cod (Gadus morhua) in response to pre-slaughter pumping stress and postmortem time. *Food Chemistry, 402*, Article 134234. https://doi.org/10.1016/j.foodchem.2022.134234

Zhang, T., Chen, C., Xie, K., Wang, J., & Pan, Z. (2021). Current state of metabolomics research in meat quality analysis and authentication. *Foods, 10*, 2388. https://doi.org/10.3390/foods10102388

Zhang, X., Han, L., Gui, L., Raza, S. H. A., Hou, S., Yang, B., … Ibrahim, S. F. (2022). Metabolome and microbiome analysis revealed the effect mechanism of different feeding modes on the meat quality of Black Tibetan sheep. *Frontiers in Microbiology, 13*, 1076675. https://doi.org/10.3389/fmicb.2022.1076675

Zhou, L., Zhang, J., Lorenzo, J. M., & Zhang, W. (2021). Effects of ultrasound emulsification on the properties of pork myofibrillar protein-fat mixed gel. *Food Chemistry, 345*, Article 128751. https://doi.org/10.1016/j.foodchem.2020.128751